



Cite this: *Nanoscale*, 2015, 7, 19403

Received 1st September 2015,
 Accepted 27th October 2015

DOI: 10.1039/c5nr05972k

www.rsc.org/nanoscale

Enhancing CVD graphene's inter-grain connectivity by a graphite promoter†

Ya-Ping Hsieh,*^a Yi-Jing Chiu^a and Mario Hofmann^b

Graphene's impact on future applications is intimately linked to advances in the synthesis of high quality materials. Chemical vapor deposition (CVD) shows great potential in this area but insufficient connectivity between single-crystalline domains deteriorates the achievable electrical and mechanical performance. We here demonstrate that the inter-grain connectivity can be significantly improved by adding a second material in the vicinity of the growth substrate. This promoter decreases the amount of structural defects that remain at the grain boundaries of conventionally grown graphene even after 6 hour growth. A two-step growth process was employed to selectively enhance the grain connectivity while maintaining an identical graphene grain morphology with and without a promoter. Graphite was found to yield the largest enhancement in the connectivity of graphene grains due to its high catalytic activity compared to other promoter materials. A novel cap-design ensured a large scale and uniform improvement of the inter-grain connectivity results which led to an enhancement of large scale carrier mobilities from $2700 \text{ cm}^2 \text{ V}^{-1} \text{ s}^{-1}$ to $4000 \text{ cm}^2 \text{ V}^{-1} \text{ s}^{-1}$ and highlights the potential of our approach to improving the connectivity of CVD-grown graphene.

Introduction

Graphene is a two-dimensional material that consists of a single atomic layer of carbon atoms.¹ Due to its unique electronic and mechanical properties, it has been heralded as an enabling material for novel electronic devices, optical components, and biological sensors.^{2,3} Breakthroughs in those areas rely on the scalable synthesis of high quality graphene

films.⁴ Chemical vapor deposition (CVD) is a promising route for achieving this goal^{5,6} and the microscopic device performance comparable to exfoliated graphene samples has been reported.^{7,8}

The performance of large-scale graphene films, however, is deteriorated by grain boundaries and defects.^{9–13} Tsen *et al.*¹⁴ observed that the connectivity between neighboring grains is the most important parameter in carrier transport and attributed differences in the growth process for increasing their connectivity by one order of magnitude. It was found that the electrochemical response of graphene was severely deteriorated by the presence of structural defects between graphene domains which expose the underlying substrate^{15–17}. Finally, failure under mechanical stress was observed to originate from weak points in the grain boundaries.^{18,19} A recent approach to overcoming these issues is to avoid polycrystallinity altogether by producing large single-crystalline grains through nucleation control.^{20,21} This method, however, is not easily scalable beyond the centimeter-size and improving the grain connectivity remains an important issue.

One determining factor for the quality of the inter-grain connection is the graphene growth kinetics. Previous reports showed that the growth rate of graphene decreases as the distance between the neighboring grains shrinks and results in unfilled areas at the grain boundaries.^{22,23} The competition between the graphene coverage and the growth rate originates from the deactivation of the catalyst substrate by the outgrowing graphene and represents a fundamental aspect of surface-catalyzed growth as observed on commonly employed Cu or Pt catalysts.²⁴

A second catalyst was found to overcome this issue through a process of distributed catalysis.²⁴ In this scheme the second catalyst acts as a promoter for the Cu-catalyst by providing carbon radicals. We here demonstrate that the use of a promoter not only improves the growth kinetics of graphene but also enhances the connectivity of neighboring grains. A two-step growth process was employed where graphene was first grown without a promoter until the maximum coverage had been achieved. Subsequent growth with a graphite promoter was

^aGraduate of Institute of Opto-Mechatronics, National Chung Cheng University, 168, University Rd., Min-Hsiung, Chia-Yi, 62102, Taiwan. E-mail: yphsieh@ccu.edu.tw

^bDepartment of Material Science and Engineering, National Cheng Kung University, Tainan, 62102, Taiwan

†Electronic supplementary information (ESI) available: Optical micrographs of oxidation tests; comparison of different characterization methods; extended characterization of graphene grown using various cap materials; large scale uniformity of graphene characterization of OM after etching. See DOI: 10.1039/c5nr05972k

found to uniformly decrease the density of structural defects across the whole sample as characterized by Raman spectroscopy and corrosion tests. The improved inter-grain connectivity results in an increase in large-scale Hall mobility from $2500 \text{ cm}^2 \text{ V}^{-1} \text{ s}^{-1}$ to $4000 \text{ cm}^2 \text{ V}^{-1} \text{ s}^{-1}$ which indicates the potential of our approach.

Experimental

Graphene synthesis was conducted on copper foil (99.8%, Alfa-Aesar, no. 46365) following previous reports.²⁵ Briefly, electrochemical polishing in an electrolyte containing H_3PO_4 (85%) was employed to control the morphology of the copper foil.²⁶ After electropolishing treatment, the copper was washed with copious amounts of deionized water and dried with N_2 . The pretreated Cu foils were then used to carry out graphene growth. First, the foils were annealed under a hydrogen atmosphere for 70 min to initiate Cu grain growth and to remove the organic residue and surface oxide. Graphene growth was conducted at $1030 \text{ }^\circ\text{C}$ in a gas mixture of H_2 (200 sccm) and CH_4 (10 sccm) for various times and rapidly cooled under 10 sccm hydrogen flow.

To characterize the coverage of graphene, both air oxidation of copper²⁷ and film-induced frustrated etching (FIFE)²² were employed. Air oxidation was performed by heating the graphene/Cu sample to $200 \text{ }^\circ\text{C}$ for 10 min using a hot plate. For FIFE-characterization graphene samples were etched by immersing the sample in ammonium persulfate (APS) (Transene, APS-100 Copper etchant) for 10 seconds, washed with deionized water and dried with N_2 . OM images were obtained afterwards for each sample and image processing was conducted to quantify the etch pit coverage.

For further analysis, graphene was transferred from Cu to SiO_2/Si wafers and quartz plates using polymethylmethacrylate (PMMA) as a supporting layer and APS as the Cu etchant.²⁸

Electrical properties were analysed on $1 \times 1 \text{ cm}$ samples in van-der-Pauw-geometry and the sheet resistance and Hall mobility were extracted. Measurement of the graphene quality using Raman spectroscopy was carried out in a home-built Raman system using a 532 nm laser with a power of 6.4 mW. 10 spectra were recorded on each sample with equal spacing and the results were averaged from individual fits.

Results and discussion

To demonstrate the influence of a promoter on the connectivity of grains, other effects of the promoter have to be limited. One important factor to consider is the morphology of graphene in the presence of a promoter. The expected increase in carbon radical concentration results in larger nucleation densities of grains which would result in smaller domain sizes and obscure the effects of the enhanced inter-grain connectivity.²⁹

We therefore designed a two-step growth process that minimizes the difference in morphology for graphene grown with and without a promoter. In the first step, graphene was grown without a promoter. The growth duration was chosen to ensure the maximum achievable graphene coverage and limit the amount of uncovered regions. In the second growth step a promoter was introduced to enhance the growth kinetics. Since this step was carried out at almost complete coverage, the nucleation of new grains is expected to be negligible and the main effect of the promoter is to enhance the connectivity of the previously grown films (Fig. 1).

We first establish the morphology of graphene grown without a promoter by analyzing the coverage of graphene using copper oxidation²⁷ and FIFE etching tests.²² Briefly, both tests reveal the presence of the graphene film by its ability to protect the underlying copper substrate from oxidation in air or from an etchant.

Both characterization techniques show an increase in graphene coverage for longer growth durations (Fig. 2(a)). Interestingly, oxidation in air shows no discoloration of the graphene-passivated copper foil after 20 minutes growth (ESI Fig. S1†) suggesting that the graphene is continuous. Exposure of the graphene/copper structure to an etchant, on the other hand, shows an under-graphene-coverage (UGC) of only 90%. This difference in coverage originates from the previously reported amplification of nanosized structural defects and openings by under-etching for FIFE.²² The sensitivity of this technique to

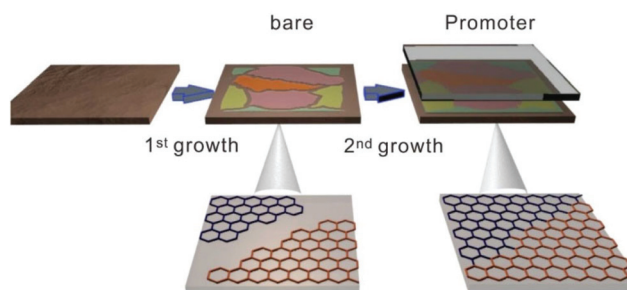


Fig. 1 Representation of the two-step growth process and its influence on the grain connectivity.

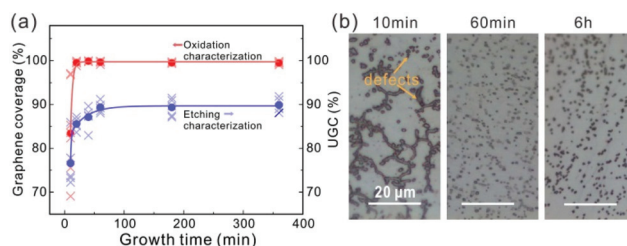


Fig. 2 Coverage of graphene vs. growth time analyzed from (a) (1) air oxidation (2) APS etching, (b) optical images of APS etched morphology after different growth durations.

graphene defects that are otherwise undetectable (Fig. S2†) is thought to originate from the difference in the interaction between graphene defects and liquid etchant compared to oxygen.³⁰

Due to its higher sensitivity to nanosized openings we subsequently focus on the FIFE etching tests and characterize the under-graphene-coverage (UGC) of copper for different growth durations. Fig. 2(a) shows that the UGC increases within the first 60 minutes but reaches a constant value of 90% that cannot be increased by prolonged growth. Even after 6 hours of growth no full coverage can be achieved. This behavior demonstrates that a limitation of graphene quality exists which originates from the previously observed decrease in graphene growth rate at high coverage due to catalyst deactivation.

We chose 60 min growth duration for the first step since it represents the maximum achievable graphene coverage and subsequently investigate the effect of the second growth step on the graphene continuity.

One concern for the proposed two-step growth process is that the exposure to air between the growth steps could deteriorate the graphene quality. We therefore compare the continuity for graphene that was grown uninterruptedly for 3 hours with graphene that was subjected to a two-step growth consisting of a one and a two-hour period. It is found that the UGC with and without interruption are virtually identical (Fig. 3(a)) and are similar to a one-hour growth step. This behavior indicates that the interruption and exposure to air does not affect the graphene quality.

We now turn to investigating the use of promoters during the second growth step to increase the graphene's continuity. For this purpose, a capping layer was positioned on top of the copper growth substrate. In order to avoid direct contact of the copper and graphite surfaces, a 200 μm graphite spacer was introduced (Fig. 3(b)).

Several capping materials were investigated for their ability to increase the graphene continuity. A quartz cap (thickness 2 mm, roughness 0.8 μm) was chosen to represent an inert material that is not expected to contribute to graphene growth.³¹ A second piece of copper foil was used to investigate previous reports on the promoting effect of the material.³² Graphite was used as a promoter due to a number of advantages over the previously used materials. First, graphite's refractory nature limits the interdiffusion during growth and no graphene growth was observed in the absence of the CH_4 precursor. Furthermore, inevitable formation of carbon layers on the promoter will not change its catalytic activity in contrast to metal promoters that have been reported to suffer from catalyst coking due to the formation of carbide or graphene layers.²⁴

Fig. 3(c) shows the resulting UGC after the second growth step was carried out with different capping materials. We observe that the quartz cap is decreasing the quality of the graphene compared to the first step and the un-capped growth. This behavior can be understood when considering the stability of graphene under the growth conditions. Previous reports found a dynamical equilibrium between adsorption and desorption of carbon atoms to the edges of graphite.³³ Especially in the presence of hydrogen gas, graphene was found to etch at high temperatures. In the case of the capped geometry, confinement effects become important and gas diffusion is hindered by wall collisions. In this regime a lower pressure exists in the capped area and desorption proceeds more efficiently than adsorption resulting in the observed decrease in graphene coverage.

The investigated copper cap, on the other hand, has a beneficial effect on the graphene coverage as seen in Fig. 3(c). This is due to the higher catalytic activity of the initially uncovered copper surface of the promoter. Consequently, carbon radicals are produced by the second Cu foil and can diffuse through the gap to interact with the already covered growth substrate. This effect, however, is limited in time because the copper cap itself will nucleate and grow graphene on similar time scales to one-step growth. Thus, the promoter becomes passivated after the first 60 minutes and does not contribute during the rest of the growth duration.

The largest improvement in continuity is observed for graphite. A 95% UCR is thought to represent the maximum achievable coverage in the presence of surface impurities.¹⁵

This observation is surprising since graphite is not commonly known to catalyze methane dehydrogenation – a prerequisite for the promoter effect.²⁴ We carried out temperature dependent growth rate measurements on individual graphene grains (Fig. 3(d)) to investigate this issue. From the Arrhenius plot, we extract an activation energy barrier of $E_A = 2.42$ eV for the graphite promoter and $E_A = 3.03$ eV for the copper promoter. The trends and values of these two barriers agree with previous reports.²⁴ This finding suggests that graphite can act as a promoter despite not being as efficient as the previously investigated Ni which exhibits an activation energy barrier of $E_A = 1.32$ eV.²⁴

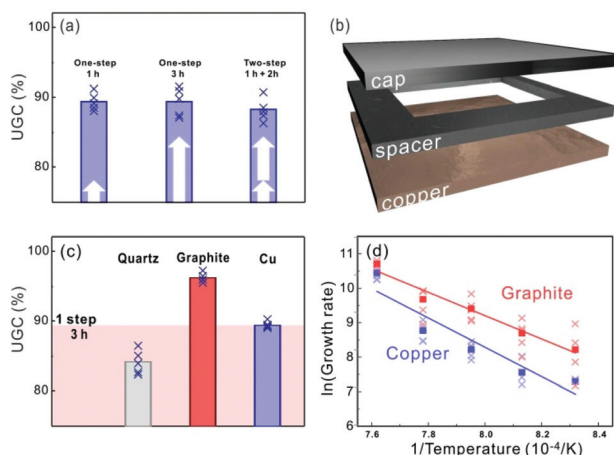


Fig. 3 (a) Coverage after APS etching vs. time for uncapped one-step and two-step growth. (b) Schematic of capped geometry, (c) comparison of coverage after APS etching using various cap materials (optical images can be found in ESI Fig. S5†), (d) growth rate for graphite and copper caps vs. temperature.

Finally, we correlate the investigated improvement in graphene continuity with enhancements in the quality of the graphene film. Fig. 4(a) shows the result of Raman spectroscopic characterization. The Raman I_D/I_G ratio, a common measure of the graphene quality, is showing a trend that is similar to the UGC results with graphite having the lowest and quartz having the highest defectiveness. This result suggests that the structural defects probed by the etching method are indeed defects in the graphene lattice and they can be healed by subsequent growth steps (more detailed optical characterization can be found in ESI Fig. S4†).

These findings are supported by the Hall mobility measurements of films produced using different cap materials (Fig. 4(a)). We observe a similar dependence of mobility on the growth process as the defectiveness with graphite caps exhibiting the highest mobility and quality. Surprisingly, the quartz capped growth exhibits a high mobility despite higher defectiveness. Future research has to elucidate whether this behavior is due to the removal of amorphous carbon that could act as neutral scatterers for carrier transport.³⁴

The observed enhancement cannot be explained by the lower porosity of the graphene film. Random voids would modify the Hall resistance according to $R_m = R_0/(1 - \epsilon)$ where ϵ is the fraction of the missing material which is smaller than the UGC and thus the mobility decrease would be less than 10%.³⁵

Characterization of the UGC and Raman I_D/I_G ratio both suggest only small improvements in the quality of graphene by 5% for etching and by 25% for Raman analysis. Despite this limited enhancement, the carrier mobility increases by 70% compared to the uncapped growth. This large change of the mobility by small variations in defectiveness demonstrates the dependence of the graphene performance on the grain connectivity.

Furthermore, a decrease in carrier concentration by 50% (ESI Fig. S3(a)†) suggests that the incompletely connected areas are the source of significant adsorption and doping induced charge transfer.

Finally, we show that the enhancement effect can be achieved on a large scale by measuring the coverage of graphene as a function of position along one 6 cm long sample (Fig. 4(b)). It can be seen that the UGC of ~96% after APS

etching is retained throughout the sample while maintaining the uniform single layer distribution (ESI Fig. S4†).

Conclusions

In conclusion, we show that graphite is a suitable promoter material for a large scale and uniform enhancement of the graphene grain connectivity. This improvement resulted in a significant increase in carrier mobility and highlights the potential of enhancing the inter-grain connectivity for high quality graphene films.

Acknowledgements

The authors acknowledge financial support by the Ministry of Science and Technology, Taiwan, R.O.C and the Industrial Technology Research Institute of Taiwan, R.O.C.

References

- 1 A. K. Geim and K. S. Novoselov, *Nat. Mater.*, 2007, **6**, 183–191.
- 2 A. C. Neto, F. Guinea, N. Peres, K. S. Novoselov and A. K. Geim, *Rev. Mod. Phys.*, 2009, **81**, 109.
- 3 I. Frank, D. M. Tanenbaum, A. Van der Zande and P. L. McEuen, *J. Vac. Sci. Technol., B*, 2007, **25**, 2558–2561.
- 4 K. S. Novoselov, V. Fal, L. Colombo, P. Gellert, M. Schwab and K. Kim, *Nature*, 2012, **490**, 192–200.
- 5 X. Li, W. Cai, J. An, S. Kim, J. Nah, D. Yang, R. Piner, A. Velamakanni, I. Jung and E. Tutuc, *Science*, 2009, **324**, 1312–1314.
- 6 B. Y. Chen, H. X. Huang, X. M. Ma, L. Huang, Z. Y. Zhang and L. M. Peng, *Nanoscale*, 2014, **6**, 15255–15261.
- 7 N. Petrone, C. R. Dean, I. Meric, A. M. van Der Zande, P. Y. Huang, L. Wang, D. Muller, K. L. Shepard and J. Hone, *Nano Lett.*, 2012, **12**, 2751–2756.
- 8 Y. R. Liang, X. L. Liang, Z. Y. Zhang, W. Li, X. Y. Huo and L. M. Peng, *Nanoscale*, 2015, **7**, 10954–10962.
- 9 R. Grantab, V. B. Shenoy and R. S. Ruoff, *Science*, 2010, **330**, 946–948.
- 10 P. Y. Huang, C. S. Ruiz-Vargas, A. M. van der Zande, W. S. Whitney, M. P. Levendorf, J. W. Kevek, S. Garg, J. S. Alden, C. J. Hustedt and Y. Zhu, *Nature*, 2011, **469**, 389–392.
- 11 G.-H. Lee, R. C. Cooper, S. J. An, S. Lee, A. van der Zande, N. Petrone, A. G. Hammerberg, C. Lee, B. Crawford and W. Oliver, *Science*, 2013, **340**, 1073–1076.
- 12 H. I. Rasool, C. Ophus, W. S. Klug, A. Zettl and J. K. Gimzewski, *Nat. Commun.*, 2013, **4**.
- 13 P. Nemes-Incze, K. J. Yoo, L. Tapasztó, G. Dobrik, J. Lábár, Z. E. Horváth, C. Hwang and L. P. Biró, *Appl. Phys. Lett.*, 2011, **99**, 023104.

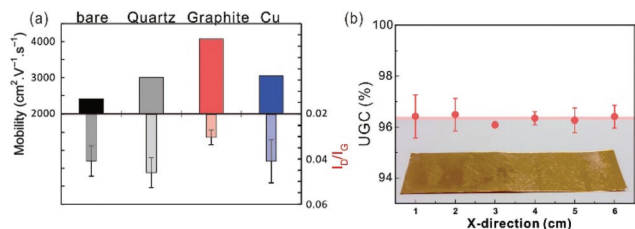


Fig. 4 (a) Comparison of the Hall mobility and Raman I_D/I_G (on the inverted scale) for different capping materials; (b) coverage after APS etching as a function of position across a 6 cm sample (inset is a photograph of the graphene/copper sample before transfer).

- 14 A. W. Tsen, L. Brown, M. P. Levendorf, F. Ghahari, P. Y. Huang, R. W. Havener, C. S. Ruiz-Vargas, D. A. Muller, P. Kim and J. Park, *Science*, 2012, **336**, 1143–1146.
- 15 Y.-P. Hsieh, M. Hofmann, K.-W. Chang, J. G. Jhu, Y.-Y. Li, K. Y. Chen, C. C. Yang, W.-S. Chang and L.-C. Chen, *ACS Nano*, 2013, **8**, 443–448.
- 16 D. A. C. Brownson and C. E. Banks, *RSC Adv.*, 2012, **2**, 5385–5389.
- 17 D. A. C. Brownson and C. E. Banks, *Phys. Chem. Chem. Phys.*, 2012, **14**, 8264–8281.
- 18 G. Rutter, J. Crain, N. Guisinger, T. Li, P. First and J. Stroscio, *Science*, 2007, **317**, 219–222.
- 19 O. V. Yazyev and S. G. Louie, *Nat. Mater.*, 2010, **9**, 806–809.
- 20 Q. Yu, L. A. Jauregui, W. Wu, R. Colby, J. Tian, Z. Su, H. Cao, Z. Liu, D. Pandey and D. Wei, *Nat. Mater.*, 2011, **10**, 443–449.
- 21 I. Vlassiouk, S. Smirnov, M. Regmi, S. P. Surwade, N. Srivastava, R. Feenstra, G. Eres, C. Parish, N. Lavrik and P. Datskos, *J. Phys. Chem. C*, 2013, **117**, 18919–18926.
- 22 M. Hofmann, Y. C. Shin, Y.-P. Hsieh, M. S. Dresselhaus and J. Kong, *Nano Res.*, 2012, **5**, 504–511.
- 23 L. Colombo, X. Li, B. Han, C. Magnuson, W. Cai, Y. Zhu and R. S. Ruoff, *ECS Trans.*, 2010, **28**, 109–114.
- 24 Y.-P. Hsieh, M. Hofmann and J. Kong, *Carbon*, 2014, **67**, 417–423.
- 25 Z. Luo, Y. Lu, D. W. Singer, M. E. Berck, L. A. Somers, B. R. Goldsmith and A. C. Johnson, *Chem. Mater.*, 2011, **23**, 1441–1447.
- 26 G. H. Han, F. Güneş, J. J. Bae, E. S. Kim, S. J. Chae, H.-J. Shin, J.-Y. Choi, D. Pribat and Y. H. Lee, *Nano Lett.*, 2011, **11**, 4144–4148.
- 27 S. Chen, L. Brown, M. Levendorf, W. Cai, S.-Y. Ju, J. Edgeworth, X. Li, C. W. Magnuson, A. Velamakanni and R. D. Piner, *ACS Nano*, 2011, **5**, 1321–1327.
- 28 J. D. Wood, G. P. Doidge, E. A. Carrion, J. C. Koepke, J. A. Kaitz, I. Datye, A. Behnam, J. Hewaparakrama, B. Aruin and Y. Chen, *Nanotechnology*, 2015, **26**, 055302.
- 29 T. Wu, G. Ding, H. Shen, H. Wang, L. Sun, D. Jiang, X. Xie and M. Jiang, *Adv. Funct. Mater.*, 2013, **23**, 198–203.
- 30 S. Garaj, W. Hubbard, A. Reina, J. Kong, D. Branton and J. Golovchenko, *Nature*, 2010, **467**, 190–193.
- 31 H. Moosberg-Bustnes, B. Lagerblad and E. Forsberg, *Mater. Struct.*, 2004, **37**, 74–81.
- 32 G. Brist, S. Hall, S. Clouser and T. Liang, *Proc. Electron. Circuits World Conv.*, 2005, **10**, 22–24.
- 33 J.-M. Simon, O.-E. Haas and S. Kjelstrup, *J. Phys. Chem. C*, 2010, **114**, 10212–10220.
- 34 Z. Ni, L. Ponomarenko, R. Nair, R. Yang, S. Anissimova, I. Grigorieva, F. Schedin, P. Blake, Z. Shen and E. Hill, *Nano Lett.*, 2010, **10**, 3868–3872.
- 35 H. J. Juretschke, R. Landauer and J. a. Swanson, *J. Appl. Phys.*, 1956, **27**, 838–838.